
Generative Pre-Trained Diffusion Paradigm for Zero-Shot Time Series Forecasting

Jiarui Yang^{1,2}, Tao Dai³, Naiqi Li², Junxi Wu^{1,2}, Peiyuan Liu², Jigang Bao²,
Jinmin Li², Haigang Zhang⁴, Shu-Tao Xia²,

¹Nankai University.

²Tsinghua Shenzhen International Graduate School, Tsinghua University.

³Shenzhen University. ⁴Shenzhen Polytechnic University.

Abstract

In recent years, generative pre-trained paradigms such as Large Language Models (LLMs) and Large Vision Models (LVMs) have achieved revolutionary advancements and widespread real-world applications. Particularly, the emergence of pre-trained LLMs-based temporal works, compared to previous deep model approaches, has demonstrated superior generalization and robustness, showcasing the potential of generative pre-trained paradigms as foundation models for time series. However, those LLMs-based works mainly focus on cross-modal research, i.e., leveraging the language capabilities of LLMs in time series contexts. Although they have achieved impressive performance, there still exist the issues of concept drift caused by differences in data distribution and inflexibility caused by misalignment of dimensions. To this end, inspired by recent work on LVMs, we reconsider the paradigm of time series modeling. In this paper, we comprehensively explore, for the first time, the effectiveness and superiority of the Generative Pre-trained Diffusion (GPD) paradigm in real-world multivariate time series forecasting (TSF). Specifically, to mitigate performance bias introduced by sophisticated networks, we propose a straightforward MLP diffusion network for unconditional modeling of time series. Then we employ a zero-shot and tuning-free method to predict (generate) future data using historical data as prompts. The GPD paradigm is established on the time series modality, effectively preventing the phenomenon of concept drift, and enabling flexible forecasting of arbitrary lengths. We demonstrate that the GPD paradigm achieves comprehensive performance and generalization comparable to current SOTA LLM-based and deep model paradigms on mainstream benchmarks and various TSF tasks. Extensive experiments validate the potential of the GPD paradigm and its assistance in future related research.

1 Introduction

In domains crucial to our daily lives such as finance, healthcare, and transportation, vast amounts of irregular time series data abound, characterized by varying lengths, features, and distributions [61, 37]. Time series forecasting (TSF) have long held significant importance and garnered considerable attention in these real-world domains [26]. In a nutshell, TSF is described as given a historical sequence $Y_H = \{y^0, y^1, \dots, y^H | y^i \in R^D\}$ of length H with D features, predicting future sequence $Y_P = \{y^{H+1}, y^{H+2}, \dots, y^L | y^i \in R^D\}$ of length P , where $L = P + H$, represents the total length.

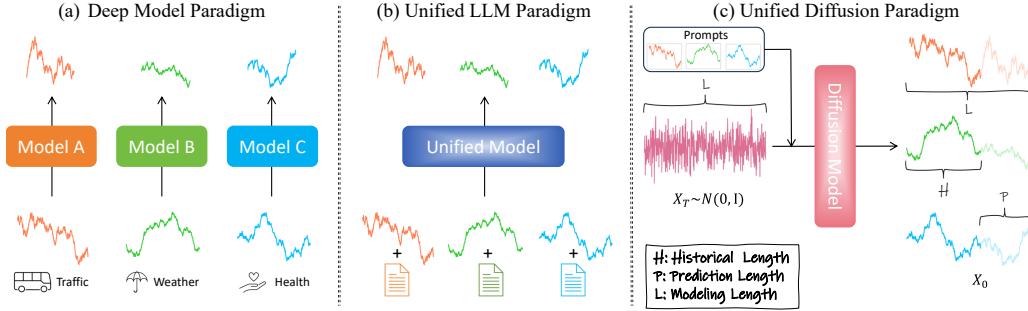


Figure 1: (a) The exclusive model establishes a singular mapping from history to future within a specific domain. (b) The unified model leverages the capabilities of LLMs and domain-specific textual instructions to differentiate and construct complex mappings. (c) The diffusion model establishes global underlying statistical characteristics across different domains. Note that paradigms (a) and (b) require retraining when altering the length of historical context. The diffusion paradigm offers flexibility in adjusting the length of historical prompts.

Confronted with the complexity of real-world time series, TSF algorithms usually require heightened generalization, flexibility, and robustness [20, 52].

Over the past decade, with the continuous development of deep networks, deep models [16, 8, 40] have achieved significant success in TSF. Particularly, the Transformer-based deep models paradigm have recently come to dominate the field [33, 67, 59]. However, the emergence of large models and large-scale data has revealed the limitations of the traditional paradigm [29]. Firstly, as depicted in Fig. 1(a), the deep models paradigm is typically trained and tested on small-scale networks and single-domain small data. This mechanism may be overly restrictive for real-world applications, resulting in compromised generalization and robustness of models. Secondly, these models usually have fixed input-output dimensions, requiring fixed-length look-back windows during both training and testing. Consequently, they struggle to handle real-world time series of irregular lengths flexibly.

Foundation models of Natural Language Processing (NLP) [54, 5] and Computer Vision (CV) [30, 3, 44] are rapidly gaining prominence, demonstrating remarkable generalization and robustness across various real-world scenarios. The inherent sequence modeling capability of LLMs naturally lends itself to time series modeling characteristics. Consequently, recent efforts [29, 15, 19, 69] in LLM-based TSF have achieved preliminary success. However, much of the LLMs-based works still follows the previous deep models paradigm. Smaller datasets and single-domain learning do not effectively showcase the superiority of LLMs in the context of time series. To address this, Liu et al. [29] propose UniTime, which empowers LLMs with cross-domain data, as shown in Fig. 1(b). UniTime is the first to validate the more robust generalization and performance brought about by cross-domain learning. The success of LLMs stems from adequately pre-training and learning universal language knowledge representations. However, recent LLMs-based works have failed to effectively address the issue of pre-trained weight distortion [46, 27], inevitably introducing the phenomenon of concept drift and consequently leading to sub-optimal performance. Moreover, due to modeling constraints, most LLMs-based methods remain inflexible, requiring fixed input and output lengths similar to deep models paradigm. Yet, a sound foundation model should be as flexible as ChatGPT in engaging in dynamic conversations, accommodating input of arbitrary lengths.

Recently, the video generation paradigm exemplified by Sora [30, 36] validates the potential of diffusion models [44, 17] in modeling multivariate time series. The application of pre-trained video generators to downstream tasks, such as video frame prediction [11, 4], is particularly inspiring to us. To this end, we rethink the modeling paradigm and explore the possibility and superiority of Generative Pre-trained Diffusion (GPD) paradigm in TSF. Firstly, as shown in Fig. 2, the GPD paradigm demonstrates comprehensive performance comparable to LLM-based and deep model paradigms. Secondly, unlike the cross-modal approach of LLMs paradigm, we construct the foundation model based on the time series modality. Therefore, our method have good interpretability, thereby avoiding conceptual drift. Finally, as shown in Fig. 1(c), the GPD paradigm can flexibly apply any historical and future lengths ($H&P$) within the maximum length L .

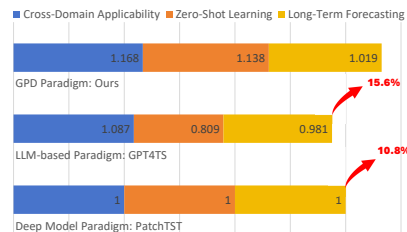


Figure 2: Comparison of comprehensive performance of different paradigms.

While there exist some temporal works based on diffusion models [42, 53, 1, 25, 13], most of them rely on additional predictors such as initial estimates provided by RNNs. This modeling approach imposes constraints on the model, compromising prior knowledge and robustness [57]. The joint training of additional predictor modules with diffusion models leads to a potential coupling between priors and predictors. This coupling results in a trade-off between diffusion denoising and predictor performance, making it challenging to effectively apply them to downstream tasks. Unlike multi-modal text or image embeddings where inputs have close semantic associations [41], the initial estimates from predictors inherently contain errors compared to ground truth, which are gradually amplified during the sampling stage. Diverging from the majority of diffusion-based temporal works, we adopt a pre-trained perspective, constructing an unconditional multivariate time series generator as the foundation model. In downstream TSF tasks, we utilize any length H of historical sequence as a prompt to generate future sequence of length P in a zero-shot manner at once. The superiority of the GPD paradigm lies in its avoidance of learning the underlying mapping between input and output, instead effectively leveraging the underlying statistical features and latent data distribution of time series data. Consequently, GPD exhibits advantages in terms of generalization and universality. We summarize the main contributions of this paper as follows:

- We propose a novel and exploratory Generative Pre-trained Diffusion (GPD) paradigm for time series analysis. Our experiments and methodology offer valuable guidance and inspiration for future related research endeavors.
- Diffusion-based method beats methods based on LLMs and deep models in multiple forecasting tasks for the first time.
- Our proposed GPD supports forecasting with arbitrary lengths of historical data, demonstrating higher flexibility and generality compared to prior methods.

2 Method

2.1 Preliminary

Denosing Diffusion Probabilistic Models (DDPMs [17, 49]) are a class of probability-based generative models that learn the mapping from high-dimensional Gaussian noise to the data distribution, enabling the generation of novel samples. From a mathematical perspective, DDPMs can be formalized as a Markov chain process [39]. Specifically, the process starts from the data distribution $X \sim q(X)$, and gradually adds Gaussian noise according to a pre-defined schedule $\{\beta_0, \dots, \beta_T\}$, generating a series of intermediate states $\{X_0, \dots, X_T\}$ defined by the conditional probability distributions $q(X_t|X_{t-1})$. Here, X_T approximates standard Gaussian noise. This process is called the forward diffusion, and it is Gaussian:

$$q(X_t|X_{t-1}) = \mathcal{N}(X_t; \sqrt{\alpha_t}X_{t-1}, (1 - \alpha_t)\mathbf{I}) \quad (1)$$

where $\alpha_t = 1 - \beta_t$. The generation process then runs in reverse order, reconstructing the data from noise, by sampling according to the inverse conditional probabilities $p_\theta(X_{t-1}|X_t)$. This process is called the reverse diffusion, and it is defined as:

$$p_\theta(X_{t-1}|X_t) = \mathcal{N}(X_{t-1}; \mu_\theta(X_t, t), \tilde{\beta}_t\mathbf{I}) \quad (2)$$

where $\tilde{\beta}_t$ is a fixed variance, and μ_θ is the mean, which contains the learnable parameter θ . Essentially, we optimize the parameter θ by minimizing the Evidence Lower Bound (ELBO [48]) of the estimated negative log-likelihood $\mathbb{E}[-\log p_\theta(X_0)]$, in order to maximize the probability of observing the training sample X_0 estimated by $p_\theta(X_0)$.

2.2 Pre-Trained Diffusion Model

We focus on exploring the potential of Generative Pre-trained Diffusion (GPD) paradigm in zero-shot time series forecasting (TSF). Therefore, to avoid performance bias introduced by sophisticated networks, we opt for a simple MLP network as a baseline for modeling. We adopt the MLP network proposed by Preechakul et al. [38] which consists of multiple MLP blocks concatenated together, with each block having a skip connection from the input. We adhere to the channel-wise independent

setting of UniTime [29] and PatchTST [33] to flexibly handle data from different domains with different feature. Relative to optimizing the ELBO, we opt for the simplified objective function [17]:

$$\mathcal{L}_{\text{simple}} = \mathbb{E}_{\Gamma, t} [\|\Gamma_{\theta}(X_t, t) - \Gamma\|_2^2] \quad (3)$$

where Γ corresponds to the noise ϵ or initial state X_0 predicted by the network.

2.3 Zero-Shot Prompt Forecasting

Regression models typically learn a deterministic and unique mapping relationship from historical data. In contrast, diffusion models can take a more global perspective $\{y^i\}_{i=1}^L$ and explore multiple approximate solutions in a broader prior space. We utilize prompts similar to those used in the image generation domain, such as video frame prediction [4] and image inpainting [50], to predict the posterior distribution at each sampling step by injecting the historical data $\{y^i\}_{i=1}^H$ as the prompt. This requires aligning the prompt distribution with the pre-trained model’s posterior distribution through posterior sampling [9]. We first apply forward diffusion to the historical prompt to add noise:

$$Y_{H_t} = \sqrt{\bar{\alpha}_t} Y_{H_0} + \sqrt{1 - \bar{\alpha}_t} \epsilon_{\theta}(X_t, t) \quad (4)$$

where $Y_{H_0} = \{y_0^i\}_{i=1}^H$ represents the GT historical sequence of length H , and ϵ_{θ} denotes the noise predicted by the pre-trained model. Then, we align the distributions through Eq. 2:

$$Y_{H_{t-1}} = p_{\theta}(Y_{H_{t-1}} | Y_{H_t}) = \mathcal{N}(Y_{H_{t-1}}; \mu_{\theta}(Y_{H_t}, t), \tilde{\beta}_t \mathbf{I}) \quad (5)$$

At each time step of diffusion sampling, we replace the corresponding sequence of the pre-trained model’s posterior distribution X_{t-1} with $Y_{H_{t-1}}$:

$$X_{H_{t-1}} =: \{x_{t-1}^i\}_{i=1}^H = Y_{H_{t-1}} \quad (6)$$

We ultimately sample a time series \hat{X}_0 of length L constructed from historical data and future predictions. In fact, our approach relies entirely on a pre-trained generative model without fine-tuning for downstream forecasting tasks. Therefore, to alleviate randomness and enhance zero-shot TSF accuracy, we perform multiple samplings and average them to obtain an unbiased estimate:

$$E[\hat{X}_0] = \sum_{i=1}^n \hat{X}_0^i \cdot p_{\theta}(\hat{X}_0^i | X_T^i) \quad (7)$$

Table 1: **Benchmarks for Different Tasks.**

Tasks	Datasets	Input Length	Output Length
Cross-Domain	ETT (4 subsets), Electricity, Weather, Exchange [23]	96	96~720
Long-term Forecasting	ETT (4 subsets), Electricity [55], Weather, Traffic [10]	512	96~720
Short-term Forecasting	Electricity, Solar [23], Traffic, Taxi [42], Wikipedia [2]	48~168	24~30
Zero-Shot	ETT (4 subsets) [67]	512	96~720

3 Experiments

3.1 Datasets and Baselines

We extensively evaluate the GPD paradigm on 9 real-world benchmarks, covering cross-domain, long-term and short-term, and zero-shot forecasting. The specific dataset settings and sequence lengths are shown in Table 1. The comprehensive baselines evaluated include:

LLM-based paradigms: *UniTime* (WWW’24) [29], *TimeLLM* (ICLR’24) [19], *LLMTime* (NeurIPS’23) [15], *GPT4TS* (NeurIPS’23) [69] and *LLMATS* (ArXiv’23) [7].

Deep model paradigms: *PatchTST* (ICLR’23) [33], *TimesNet* (ICLR’23) [60], *DLinear* (AAAI’23) [64], *FEDformer* (ICML’22), *Autoformer* (NeurIPS’21) [59], *Informer* (AAAI’21) [67] and *Pyraformer* (ICLR’21) [28].

Diffusion paradigms: *LDT* (AAAI’24) [13], *D³VAE* [25] (NeurIPS’22), *SSSD* (TML’22) [1], *CSDI* (NeurIPS’21) [53] and *TimeGrad* (ICML’21) [42].

Table 2: **Cross-doman forecasting performance comparisons.** Avg is averaged over all predictive lengths. We highlight the best performance across datasets with boldface to the left of the double vertical lines for the cross-dataset trained models, and we boldface and underscore the best overall performance on the entire row.

Method	Models Trained Across Datasets								Models Trained on Each Dataset														
	Ours		UniTime		GPT4TS [†]		PatchTST [†]		GPT4TS*		PatchTST*		TimesNet		DLinear		FEDformer		Autoformer		Informer		
	MSE	MAE	MSE	MAE	MSE	MAE	MSE	MAE	MSE	MAE	MSE	MAE	MSE	MAE	MSE	MAE	MSE	MAE	MSE	MAE	MSE	MAE	
ETTm1	96	0.465	0.458	0.322	0.363	0.509	0.463	0.927	0.604	0.335	0.369	0.344	0.373	0.338	0.375	0.345	0.372	0.379	0.419	0.505	0.475	0.672	0.571
	192	0.493	0.473	0.366	0.387	0.537	0.476	0.964	0.620	0.374	0.385	0.367	0.386	0.374	0.387	0.380	0.389	0.426	0.441	0.553	0.496	0.795	0.669
	336	0.508	0.481	0.398	0.407	0.564	0.488	1.041	0.656	0.407	0.406	0.392	0.407	0.410	0.411	0.413	0.413	0.445	0.459	0.621	0.537	1.212	0.871
	720	0.552	0.504	0.454	0.440	0.592	0.504	0.950	0.636	0.469	0.442	0.464	0.442	0.478	0.450	0.474	0.453	0.543	0.490	0.671	0.561	1.166	0.823
	Avg	0.505	0.479	0.385	0.399	0.551	0.483	0.971	0.629	0.396	0.401	0.392	0.402	0.400	0.406	0.403	0.407	0.448	0.452	0.588	0.517	0.961	0.734
ETTm2	96	0.221	0.295	0.183	0.266	0.229	0.304	0.240	0.318	0.190	0.275	0.177	0.260	0.187	0.267	0.193	0.292	0.203	0.287	0.255	0.339	0.365	0.453
	192	0.278	0.329	0.251	0.310	0.287	0.338	0.301	0.352	0.253	0.313	0.246	0.305	0.249	0.309	0.284	0.362	0.269	0.328	0.281	0.340	0.533	0.563
	336	0.332	0.359	0.319	0.351	0.337	0.367	0.367	0.391	0.321	0.360	0.305	0.343	0.321	0.351	0.369	0.427	0.325	0.366	0.339	0.372	1.363	0.887
	720	0.423	0.409	0.420	0.410	0.430	0.416	0.451	0.432	0.411	0.406	0.410	0.405	0.408	0.403	0.554	0.522	0.421	0.415	0.433	0.432	3.379	1.338
	Avg	0.314	0.348	0.293	0.334	0.321	0.356	0.340	0.373	0.294	0.339	0.285	0.328	0.291	0.333	0.350	0.401	0.305	0.349	0.327	0.371	1.410	0.810
ETTh1	96	0.384	0.395	0.397	0.418	0.449	0.424	0.409	0.403	0.398	0.424	0.404	0.413	0.384	0.402	0.386	0.400	0.376	0.419	0.449	0.459	0.865	0.713
	192	0.424	0.416	0.434	0.439	0.503	0.453	0.467	0.444	0.449	0.427	0.454	0.440	0.436	0.429	0.437	0.432	0.420	0.448	0.500	0.482	1.008	0.792
	336	0.451	0.440	0.468	0.457	0.540	0.477	0.509	0.472	0.492	0.466	0.497	0.462	0.491	0.469	0.481	0.459	0.459	0.465	0.521	0.496	1.107	0.809
	720	0.476	0.463	0.469	0.477	0.515	0.489	0.503	0.485	0.487	0.483	0.496	0.481	0.521	0.500	0.519	0.516	0.506	0.507	0.514	0.512	1.181	0.865
	Avg	0.434	0.430	0.442	0.448	0.502	0.461	0.472	0.451	0.457	0.450	0.463	0.449	0.458	0.450	0.456	0.452	0.440	0.460	0.496	0.487	1.040	0.795
ETTh2	96	0.255	0.320	0.296	0.345	0.303	0.349	0.314	0.361	0.312	0.360	0.312	0.358	0.340	0.374	0.333	0.387	0.358	0.397	0.346	0.388	3.755	1.525
	192	0.316	0.359	0.374	0.394	0.391	0.399	0.407	0.411	0.387	0.405	0.397	0.408	0.402	0.414	0.477	0.476	0.429	0.439	0.456	0.452	5.602	1.931
	336	0.358	0.394	0.415	0.427	0.422	0.428	0.437	0.443	0.424	0.437	0.435	0.440	0.452	0.452	0.594	0.541	0.496	0.487	0.482	0.486	4.721	1.835
	720	0.419	0.436	0.425	0.444	0.429	0.449	0.434	0.448	0.433	0.453	0.436	0.449	0.462	0.468	0.831	0.657	0.463	0.474	0.515	0.511	3.647	1.625
	Avg	0.337	0.377	0.378	0.403	0.386	0.406	0.398	0.416	0.389	0.414	0.395	0.414	0.414	0.427	0.559	0.515	0.437	0.449	0.450	0.459	4.431	1.729
Electricity	96	0.200	0.298	0.196	0.287	0.232	0.321	0.198	0.290	0.197	0.290	0.186	0.269	0.168	0.272	0.197	0.282	0.193	0.308	0.201	0.317	0.274	0.368
	192	0.205	0.303	0.199	0.291	0.234	0.325	0.202	0.293	0.201	0.292	0.190	0.273	0.184	0.289	0.196	0.285	0.201	0.315	0.222	0.334	0.296	0.386
	336	0.229	0.321	0.214	0.305	0.249	0.338	0.223	0.318	0.217	0.309	0.206	0.290	0.198	0.300	0.209	0.301	0.214	0.329	0.231	0.338	0.300	0.394
	720	0.268	0.353	0.254	0.335	0.289	0.366	0.259	0.341	0.253	0.339	0.247	0.322	0.220	0.320	0.245	0.333	0.246	0.355	0.254	0.361	0.373	0.439
	Avg	0.225	0.319	0.216	0.305	0.251	0.338	0.221	0.311	0.217	0.308	0.207	0.289	0.192	0.295	0.212	0.300	0.214	0.327	0.227	0.338	0.311	0.397
Weather	96	0.202	0.251	0.171	0.214	0.212	0.251	0.213	0.260	0.203	0.244	0.177	0.218	0.172	0.220	0.196	0.255	0.217	0.296	0.266	0.336	0.300	0.384
	192	0.250	0.289	0.217	0.254	0.261	0.288	0.269	0.300	0.247	0.277	0.222	0.259	0.219	0.261	0.237	0.296	0.276	0.336	0.307	0.367	0.598	0.544
	336	0.299	0.321	0.274	0.293	0.313	0.324	0.330	0.341	0.297	0.311	0.277	0.297	0.280	0.306	0.283	0.335	0.339	0.380	0.359	0.395	0.578	0.523
	720	0.380	0.368	0.351	0.343	0.386	0.372	0.404	0.389	0.368	0.356	0.352	0.347	0.365	0.359	0.345	0.381	0.403	0.428	0.419	0.428	1.059	0.741
	Avg	0.283	0.307	0.253	0.276	0.293	0.309	0.304	0.323	0.279	0.297	0.257	0.280	0.259	0.287	0.265	0.317	0.309	0.360	0.338	0.382	0.634	0.548
Exchange	96	0.131	0.269	0.086	0.209	0.142	0.261	0.137	0.260	0.091	0.212	0.109	0.236	0.107	0.234	0.088	0.218	0.148	0.278	0.197	0.323	0.847	0.752
	192	0.208	0.344	0.174	0.299	0.224	0.339	0.222	0.341	0.183	0.304	0.205	0.327	0.226	0.344	0.176	0.315	0.271	0.380	0.300	0.369	1.204	0.895
	336	0.309	0.436	0.319	0.408	0.377	0.448	0.372	0.447	0.328	0.417	0.356	0.436	0.367	0.448	0.313	0.427	0.460	0.500	0.509	0.524	1.672	1.036
	720	0.476	0.554	0.875	0.701	0.939	0.736	0.912	0.727	0.880	0.704	0.888	0.716	0.964	0.746	0.839	0.695	1.195	0.841	1.447	0.941	2.478	1.310
	Avg	0.281	0.401	0.364	0.404	0.421	0.446	0.411	0.444	0.371	0.409	0.390	0.429	0.416	0.443	0.354	0.414	0.519	0.500	0.613	0.539	1.550	0.998
1 st Count	22		22		0		0		2		13		8		1		2		0		0		

3.2 Implementation Details

All experiments are conducted using the diffusion network from [38], which consists of 20 MLP layers, with each layer having a hidden dimension of 2048. The number of diffusion steps is set to 200. During the pre-training stage, the model is trained on a 40G A100 GPU. For long and short-term forecasting tasks, the batch size is set to 1024 for the ETT, Weather, Solar, and Exchange datasets, and 128 or less for the remaining datasets, with a uniform iteration count of 100k. For cross-domain training, the batch size is set to 32, and the iteration count is 500k. All experiments use the Adam [22] optimizer with a learning rate of 10e-4 and the EMA rate of 0.9999 to optimize the parameters [12]. During the pre-training phase, the input length equals the historical length plus the maximum future length. For instance, for tasks with historical length 512 and different prediction horizons $H = \{96, 192, 336, 720\}$, the input length to the pre-trained model is $512+720=1232$. During testing, given 512 lengths of historical data, the model directly generates future data with a maximum length of 720. For items shorter than 720, slicing is employed for comparison. Notable that due to the DropLast [35] setting in the code, different batch sizes among methods lead to different testset lengths. We strictly ensure that the length of testsets in the comparison is consistent.

Table 3: **Long-term forecasting results.** All results are averaged from four different forecasting horizons {96, 192, 336, 720}. **Red** and **blue** indicates the best and the second best performance.

Methods	Ours	TimeLLM	LLM4TS	GPT4TS	DLinear	PatchTST	FEDformer	Autoformer	Informer	Pyraformer
Metric	MSE MAE	MSE MAE	MSE MAE	MSE MAE	MSE MAE	MSE MAE	MSE MAE	MSE MAE	MSE MAE	MSE MAE
ETTh1	0.391 0.423	0.408 0.423	0.404 0.418	0.428 0.426	0.423 0.438	0.413 0.461	0.440 0.677	0.496 0.487	1.040 0.795	0.827 0.703
ETTh2	0.300 0.365	0.334 0.383	0.331 0.383	0.355 0.395	0.431 0.447	0.370 0.379	0.437 0.449	0.450 0.459	4.431 1.729	0.829 0.703
ETTh1	0.349 0.377	0.329 0.372	0.343 0.378	0.352 0.383	0.357 0.379	0.351 0.381	0.448 0.452	0.588 0.517	0.961 0.734	0.691 0.607
ETTh2	0.262 0.314	0.251 0.313	0.251 0.313	0.267 0.326	0.267 0.334	0.255 0.315	0.305 0.349	0.327 0.371	1.410 0.810	1.498 0.869
Weather	0.234 0.289	0.225 0.257	0.223 0.260	0.237 0.271	0.249 0.300	0.226 0.264	0.310 0.360	0.338 0.382	0.634 0.521	0.815 0.717
Electricity	0.165 0.273	0.158 0.252	0.159 0.253	0.167 0.263	0.166 0.264	0.164 0.253	0.214 0.327	0.227 0.338	0.311 0.397	0.382 0.445
Traffic	0.393 0.279	0.388 0.264	0.401 0.273	0.414 0.295	0.437 0.264	0.391 0.264	0.611 0.376	0.628 0.379	0.764 0.416	1.176 0.469

Table 4: **Zero-shot forecasting results.** All results are averaged from four different forecasting horizons {96, 192, 336, 720}. **Red** and **blue** indicates the best and the second best performance.

Methods	Ours	TimeLLM	LLMTime	GPT4TS	DLinear	PatchTST	TimesNet	Autoformer
Metric	MSE MAE	MSE MAE	MSE MAE	MSE MAE	MSE MAE	MSE MAE	MSE MAE	MSE MAE
ETTh1 → ETTh2	0.303 0.368	0.353 0.387	0.992 0.708	0.406 0.422	0.493 0.488	0.380 0.405	0.421 0.431	0.582 0.548
ETTh1 → ETTm2	0.311 0.367	0.273 0.340	1.867 0.869	0.325 0.363	0.415 0.452	0.314 0.360	0.327 0.361	0.457 0.483
ETTh2 → ETTh1	0.446 0.456	0.479 0.474	1.961 0.981	0.757 0.578	0.703 0.574	0.565 0.513	0.865 0.621	0.757 0.608
ETTh2 → ETTm2	0.316 0.364	0.272 0.341	1.867 0.869	0.335 0.370	0.328 0.386	0.325 0.365	0.342 0.376	0.366 0.411
ETTh1 → ETTh2	0.333 0.389	0.381 0.412	0.992 0.708	0.433 0.439	0.464 0.475	0.439 0.438	0.457 0.454	0.470 0.479
ETTh1 → ETTm2	0.266 0.317	0.268 0.320	1.867 0.869	0.313 0.348	0.335 0.389	0.296 0.334	0.322 0.354	0.469 0.484
ETTh2 → ETTh2	0.311 0.369	0.354 0.400	0.992 0.708	0.435 0.443	0.455 0.471	0.409 0.425	0.435 0.443	0.423 0.439
ETTh2 → ETTm1	0.384 0.404	0.414 0.438	1.933 0.984	0.769 0.567	0.649 0.537	0.568 0.492	0.769 0.567	0.755 0.591

3.3 Cross-Domain Time Series Forecasting

The cross-domain forecasting follows the experimental setup of UniTime [29]. Table 2 is copied from UniTime and presents the overall performance. Two vertical lines are used to demarcate the table. The left side shows the results of cross-domain training, with forecasting horizons slices at the maximum prediction length. The data on the right side comes from the officially provided results of training models separately for each specific length and dataset. Our method achieves comparable performance to the SOTA UniTime. Notably, UniTime introduces domain priors for cross-domain modeling, i.e., distinguishing different domains during training and testing based on the text descriptions of each dataset. To ensure experimental integrity and explore the diffusion model’s ability to model complex distributions, we do not introduce conditions for distinguishing domains. In comparison with the SOTA LLMs-based paradigm GPT4TS [69] and deep models paradigm PatchTST [33] (both without introducing domain priors), GPD outperforms them comprehensively, suggesting the potential of the GPD paradigm as a fundamental and unified model from the side.

3.4 Long and Short-Term Time Series Forecasting

Long-range: Following the settings and results for long-range forecasting in TimeLLM [19] and LLM4TS [7], we pretrain the model for specific datasets. Table 3 reports the average performance comparison of our method with LLMs-based and deep models paradigm [68, 59, 67, 28] in different horizons. Overall quantification is provided in Appendix.

Short-range: Due to the current absence of diffusion-based methods in long-range forecasting, we follow the settings and results of LDT [13] for short-term forecasting and compare with similar works [42, 53, 1, 25]. Table 5 reports that our method outperforms the SOTA diffusion paradigm.

3.5 Zero-Shot Forecasting

Zero-shot forecasting is defined as a model trained on dataset A being used to predict an unseen dataset B . Following the experiments in TimeLLM, we perform a comprehensive zero-shot learning on the ETT dataset, as shown in Table 4. Based on long-term forecasting, we discover an interesting phenomenon. Under traditional mechanisms, although we are slightly inferior to TimeLLM, our zero-shot learning capability significantly surpasses that of TimeLLM [19]. Regression models primarily learn the mapping between historical and future data within the dataset. In the context of zero-shot

	Solar	Electricity	Traffic	Taxi	Wikipedia
Method	MSE				
TimeGrad	9.9e2	2.1e5	4.6e-4	2.4e	3.1e7
CSDI	9.4e2	2.4e5	4.4e-4	-	-
SSSD	5.4e2	2.3e5	4.5e-4	2.3e	2.99e7
D ³ VAE	9.2e2	2.4e5	4.5e-4	2.4e	3.2e7
LDT	7.7e2	1.6e5	4.1e-4	2.2e	2.92e7
Ours	4.1e2	1.4e5	3.3e-4	1.9e	2.32e7

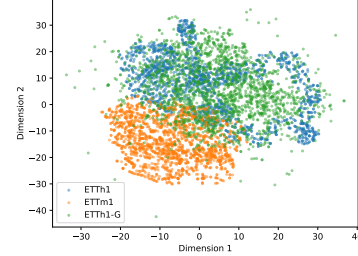


Table 5: Quantitative comparison of different diffusion-based methods in short-term forecasting

Figure 3: t-SNE Visualization of GPD modeling capability.

learning, the mapping learned by the model on dataset A may lead to suboptimal generalization performance on dataset B . In contrast, GPD paradigms model the underlying patterns and structures of time series data, thereby providing rich prior information that facilitates superior generalization.

4 Model Analysis

In this section, we conduct numerous analysis experiments on model pre-training and diffusion sampling to explore the impact of various components on the performance of zero-shot TSF. In Appendix B and C, we additionally demonstrate the zero-shot imputation and classification capabilities of proposed GPD paradigm.

Distribution Matching: We utilize a diffusion model pre-trained on the ETTh1 dataset to randomly generate 2000 samples. Subsequently, we randomly sample 2000 samples from both ETTh1 and ETTh1 datasets and employ t-SNE to visualize the data distribution. As depicted in Fig. 3, GPD exhibits robust distribution modeling capability, which is crucial for downstream tasks. Unlike current cross-modal approaches based on LLMs that may introduce concept drift phenomena, GPD offers better interpretability for modeling temporal modalities.

Sampling Steps and Prediction Strategy: The number of diffusion sampling steps directly affects the model’s inference time. We find that excessively high sampling steps may increase the transition error at each step, which is particularly evident in predicting ϵ_θ , as shown in Fig. 4(a). Conversely, the X_θ prediction mode exhibits more stability. However, both modes indicate that excessive sampling steps do not improve model performance, hence a range between 50 to 200 is a reasonable choice. In addition, Table 6 shows the comparison of different prediction models, and X_θ mode is usually better.

Sample Averaging: Due to GPD’s lack of fine-tuning the pre-trained model for forecasting tasks and relying entirely on prior knowledge from the pure generative model, results from single sampling exhibit significant randomness. As depicted in Fig. 5, we explore the MSE and MAE of different samples with varying numbers of sampling for the same time series. It can be observed that with an increase in the number of sampling, the randomness bias tends to stabilize. When the sampling number exceed 5, the bias between different samples rapidly converges to a small range. To achieve better performance, we set a uniform sampling number of 50 in all experiments, where the performance bias does not exceed 5% compared to a sampling number of 5.

Instance Normalization: Instance normalization (IN), as demonstrated by RevIN [21] in many previous methods, effectively enhances forecasting performance. However, diffusion models are designed to model noisy data directly, making it challenging to incorporate IN into the denoiser. We introduce IN through data preprocessing. For instance, for input data of length L , we normalize the data using the mean and variance of sub-sequences of length H or entire sequences. During sampling, we denormalize the predicted results using the mean and variance of the historical sequence. However, we find that the effectiveness of IN during the training process is marginal. Therefore, we propose sampling IN, which does not introduce IN during the training process but incorporates it during sampling. Across multiple datasets, sampling IN outperforms or is on par with using IN and not using IN, as shown in Fig. 6. This is because incorporating historical sequences as prompts into the posterior distribution affects the pre-trained distribution. Sampling IN reduces the impact on the distribution while ensuring modeling of the original data distribution.

Flexible Forecasting of Arbitrary Lengths: Addressing the complex forecasting needs of the real-world requires exceptional algorithmic flexibility. GPD demonstrates remarkable flexibility,

Table 6: Quantitative comparison of different prediction modes in long-range forecasting task.

Mode	ETTh1		ETTh2		ETTm1		ETTm2		Electricity		Weather		Traffic	
	MSE	MAE	MSE	MAE	MSE	MAE	MSE	MAE	MSE	MAE	MSE	MAE	MSE	MAE
ϵ_θ	0.391	0.423	0.300	0.365	0.375	0.417	0.296	0.341	0.176	0.275	0.237	0.280	0.393	0.279
X_θ	0.423	0.447	0.349	0.392	0.349	0.377	0.262	0.314	0.166	0.263	0.234	0.289	0.396	0.284

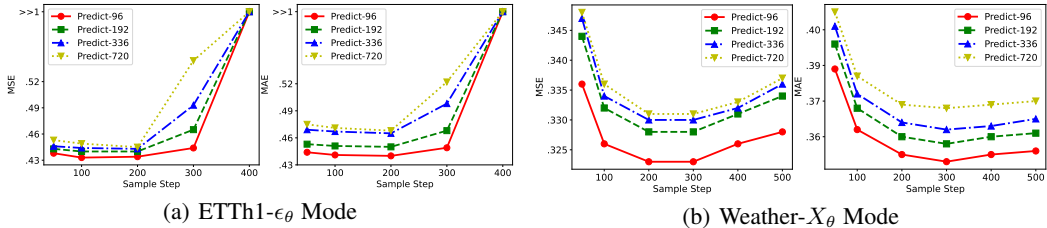


Figure 4: The impact of different sampling step settings and prediction strategies on forecasting performance. $\gg 1$ indicates that the metric is far greater than one.

which is unattainable in previous works. As shown in Fig. 7, we visualize the forecasting results of an arbitrary-length future sequence P from an arbitrary-length historical sequence H , simplified as $H \rightarrow P$. Notably, the above experiments are based on the same pre-trained model. In contrast, previous methods require training dedicated models separately for different lengths of H and P .

5 Related Works

5.1 Large Language Models for Time Series

Recently emerged works on LLMs for time series can be categorized into two pre-trained paradigms: Fine-tuning LLMs’ powerful linguistic reasoning capabilities for time series modeling. And training a dedicated time series base model from scratch.

Pre-trained LLMs. GPT4TS [69] pioneers the validation of the pre-trained paradigm’s feasibility and universality. TEMPO [6] infuses more information into pre-trained LLM by decomposing the complex interactions between trend, seasonal, and residual components during fine-tuning. Additionally, numerous efforts are devoted to aligning natural language with time series. LLTime [15] actively aligns time series data with natural language to leverage LLMs’ zero-shot logical inference capabilities. TimeLLM [19] reprograms pre-trained LLMs by adjusting the time series modality using text prompts. These methods preserve the integrity of LLMs. Furthermore, some works align modalities while fine-tuning to pursue better performance. S²IP-LLM [34] aligns the semantic space with time series embedding and predicts future based on prompts learned from the joint space. LLaTA [27] addresses the non-aligned modality between pre-trained LLMs and time series via knowledge distillation.

Time series foundation models. Another attempt is to draw inspiration from foundation models in other fields, such as NLP [41, 5] and CV [30, 44], to construct foundation models for time series. The key challenge lies in establishing robust mappings across sequential data from different feature domains. TimeGPT [14] employs large-scale Transformer trained on massive datasets to enhance robustness. Lag-Llama [43] explores using lags as covariates in a pure decoder Transformer pre-trained on large corpora of diverse time series data across multiple domains.

5.2 Diffusion Models for Time Series

TimeGrad [42] first proposes combining DDPM and RNN for multivariate time series forecasting, recursively predicting in an autoregressive manner. ScoreGrad [62] is built on score matching, utilizing a diffusion model to assist an RNN-like module in step-by-step prediction. We acknowledge that diffusion models are also iterative models, and combining autoregressive and diffusion approaches often incurs high computational costs and accumulated errors [57]. To address this, DiffSTG [58] combines spatial-temporal graphs and DDPM to propose a non-autoregressive framework, utilizing spatial-temporal graphs to guide the diffusion model in modeling spatial-temporal correlations.

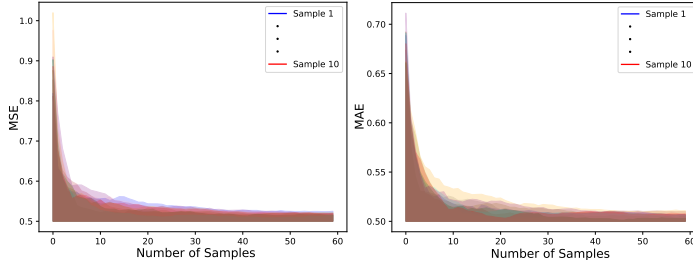


Figure 5: Analysis of Average Sampling Times.

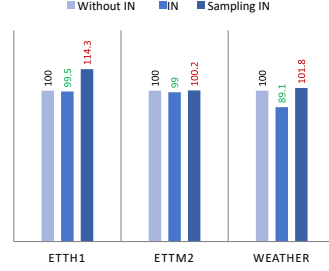


Figure 6: Normalization Analysis.

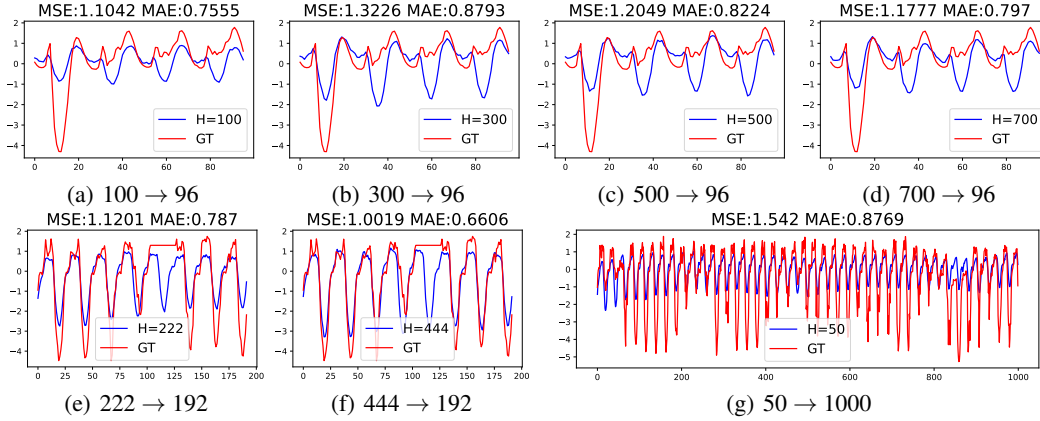


Figure 7: Visualization of Flexible Forecasting Results.

CSDI [53] and SSSD [1] introduce conditions into diffusion networks and train a conditional diffusion model with inductive bias losses. TimeDiff [47] models future data conditioned on historical data, then predicts future data in one shot through diffusion sampling. Most condition-guided methods rely on the initial prediction from the predictor, which is unfavorable for constructing fundamental and unified models. Additionally, some works attempt to leverage pre-trained diffusion paradigms. Feng et al. [13] propose a Latent Diffusion Transformer (LDT) framework, a multivariate time series diffusion model that generates realistic multivariate time stamps guided by self-conditioning. Diffusion-TS [63] combines seasonal-trend decomposition and denoising sample reconstruction to build an unconditional model, then utilizes a classifier to guide conditional tasks.

6 Conclusion and Discussion

Conclusion. We explore and propose a novel Generative Pre-trained Diffusion (GPD) paradigm for zero-shot TSF. In various real-world forecasting tasks, GPD demonstrates superior performance, surpassing methods based on LLMs and deep models for the first time. Compared to previous methods, our method is more general, versatile, and flexible. Extensive experiments and analyses validate the potential of the GPD paradigm and lay the foundation for future work.

Discussion and Limitations. Firstly, the current field of time series is not as thriving as the NLP or CV fields, lacking large-scale models and multi-modal datasets [56, 51, 45], among other resources. This somewhat limits the diversity and development within the time series domain. Although we validate the effectiveness of the GPD paradigm, its generality requires further verification. For instance, the scaling ability, multi-modal integration, and controllability need to be explored further. Secondly, fine-tuning techniques for diffusion models, such as ControlNet [65] and Adapter [32, 66], have achieved significant success in other fields. Future exploration can focus on more downstream tasks. Furthermore, the use of simple baseline may led to sub-optimal performance, thus designing superior diffusion networks for time series is necessary. Lastly, similar to diffusion-based methods in other fields, our method does not have an advantage in speed compared to end-to-end models. We found that adopting acceleration strategies [49] seriously impacts performance, possibly due to the limited modeling capability of MLP or the lack of fine-tuning for downstream tasks.

References

- [1] Juan Miguel Lopez Alcaraz and Nils Strodthoff. Diffusion-based time series imputation and forecasting with structured state space models. *arXiv preprint arXiv:2208.09399*, 2022.
- [2] A. Alexandrov, K. Benidis, M. Bohlke-Schneider, V. Flunkert, J. Gasthaus, T. Januschowski, D. C. Maddix, S. Rangapuram, D. Salinas, J. Schulz, L. Stella, A. C. Türkmen, and Y. Wang. GluonTS: Probabilistic Time Series Modeling in Python. *arXiv preprint arXiv:1906.05264*, 2019.
- [3] Yutong Bai, Xinyang Geng, Karttikeya Mangalam, Amir Bar, Alan Yuille, Trevor Darrell, Jitendra Malik, and Alexei A Efros. Sequential modeling enables scalable learning for large vision models. *arXiv preprint arXiv:2312.00785*, 2023.
- [4] Andreas Blattmann, Tim Dockhorn, Sumith Kulal, Daniel Mendelevitch, Maciej Kilian, Dominik Lorenz, Yam Levi, Zion English, Vikram Voleti, Adam Letts, et al. Stable video diffusion: Scaling latent video diffusion models to large datasets. *arXiv preprint arXiv:2311.15127*, 2023.
- [5] Tom Brown, Benjamin Mann, Nick Ryder, Melanie Subbiah, Jared D Kaplan, Prafulla Dhariwal, Arvind Neelakantan, Pranav Shyam, Girish Sastry, Amanda Askell, et al. Language models are few-shot learners. *Advances in neural information processing systems*, 33:1877–1901, 2020.
- [6] Defu Cao, Furong Jia, Sercan O Arik, Tomas Pfister, Yixiang Zheng, Wen Ye, and Yan Liu. Tempo: Prompt-based generative pre-trained transformer for time series forecasting. *arXiv preprint arXiv:2310.04948*, 2023.
- [7] Ching Chang, Wen-Chih Peng, and Tien-Fu Chen. Llm4ts: Two-stage fine-tuning for time-series forecasting with pre-trained llms. *arXiv preprint arXiv:2308.08469*, 2023.
- [8] Zonglei Chen, Minbo Ma, Tianrui Li, Hongjun Wang, and Chongshou Li. Long sequence time-series forecasting with deep learning: A survey. *Information Fusion*, 97:101819, 2023.
- [9] Jooyoung Choi, Sungwon Kim, Yonghyun Jeong, Youngjune Gwon, and Sungroh Yoon. Ilvr: Conditioning method for denoising diffusion probabilistic models. In *2021 IEEE/CVF International Conference on Computer Vision (ICCV)*, pages 14347–14356. IEEE, 2021.
- [10] Marco Cuturi. PEMS-SF. UCI Machine Learning Repository, 2011. DOI: <https://doi.org/10.24432/C52G70>.
- [11] Aram Davtyan, Sepehr Sameni, and Paolo Favaro. Efficient video prediction via sparsely conditioned flow matching. In *Proceedings of the IEEE/CVF International Conference on Computer Vision*, pages 23263–23274, 2023.
- [12] Prafulla Dhariwal and Alexander Nichol. Diffusion models beat gans on image synthesis. *Advances in neural information processing systems*, 34:8780–8794, 2021.
- [13] Shibo Feng, Chunyan Miao, Zhong Zhang, and Peilin Zhao. Latent diffusion transformer for probabilistic time series forecasting. In *Proceedings of the AAAI Conference on Artificial Intelligence*, volume 38, pages 11979–11987, 2024.
- [14] Azul Garza and Max Mergenthaler-Canseco. Timegpt-1. *arXiv preprint arXiv:2310.03589*, 2023.
- [15] Nate Gruver, Marc Finzi, Shikai Qiu, and Andrew G Wilson. Large language models are zero-shot time series forecasters. *Advances in Neural Information Processing Systems*, 36, 2024.
- [16] Hansika Hewamalage, Christoph Bergmeir, and Kasun Bandara. Recurrent neural networks for time series forecasting: Current status and future directions. *International Journal of Forecasting*, 37(1):388–427, 2021.
- [17] Jonathan Ho, Ajay Jain, and Pieter Abbeel. Denoising diffusion probabilistic models. *Advances in neural information processing systems*, 33:6840–6851, 2020.

- [18] Robert A Jacobs, Michael I Jordan, Steven J Nowlan, and Geoffrey E Hinton. Adaptive mixtures of local experts. *Neural computation*, 3(1):79–87, 1991.
- [19] Ming Jin, Shiyu Wang, Lintao Ma, Zhixuan Chu, James Y Zhang, Xiaoming Shi, Pin-Yu Chen, Yuxuan Liang, Yuan-Fang Li, Shirui Pan, et al. Time-llm: Time series forecasting by reprogramming large language models. *arXiv preprint arXiv:2310.01728*, 2023.
- [20] Ieabeling Kaastra and Milton Boyd. Designing a neural network for forecasting financial and economic time series. *Neurocomputing*, 10(3):215–236, 1996.
- [21] Taesung Kim, Jinhee Kim, Yunwon Tae, Cheonbok Park, Jang-Ho Choi, and Jaegul Choo. Reversible instance normalization for accurate time-series forecasting against distribution shift. In *International Conference on Learning Representations*, 2021.
- [22] Diederik P Kingma and Jimmy Ba. Adam: A method for stochastic optimization. *arXiv preprint arXiv:1412.6980*, 2014.
- [23] Guokun Lai, Wei-Cheng Chang, Yiming Yang, and Hanxiao Liu. Modeling long-and short-term temporal patterns with deep neural networks. In *The 41st international ACM SIGIR conference on research & development in information retrieval*, pages 95–104, 2018.
- [24] Alexander C Li, Mihir Prabhudesai, Shivam Duggal, Ellis Brown, and Deepak Pathak. Your diffusion model is secretly a zero-shot classifier. In *Proceedings of the IEEE/CVF International Conference on Computer Vision*, pages 2206–2217, 2023.
- [25] Yan Li, Xinjiang Lu, Yaqing Wang, and Dejing Dou. Generative time series forecasting with diffusion, denoise, and disentanglement. *Advances in Neural Information Processing Systems*, 35:23009–23022, 2022.
- [26] Bryan Lim and Stefan Zohren. Time-series forecasting with deep learning: a survey. *Philosophical Transactions of the Royal Society A*, 379(2194):20200209, 2021.
- [27] Peiyuan Liu, Hang Guo, Tao Dai, Naiqi Li, Jigang Bao, Xudong Ren, Yong Jiang, and Shu-Tao Xia. Taming pre-trained llms for generalised time series forecasting via cross-modal knowledge distillation. *arXiv preprint arXiv:2403.07300*, 2024.
- [28] Shizhan Liu, Hang Yu, Cong Liao, Jianguo Li, Weiyao Lin, Alex X Liu, and Schahram Dustdar. Pyraformer: Low-complexity pyramidal attention for long-range time series modeling and forecasting. In *International conference on learning representations*, 2021.
- [29] Xu Liu, Junfeng Hu, Yuan Li, Shizhe Diao, Yuxuan Liang, Bryan Hooi, and Roger Zimmermann. Unitime: A language-empowered unified model for cross-domain time series forecasting. *arXiv preprint arXiv:2310.09751*, 2023.
- [30] Yixin Liu, Kai Zhang, Yuan Li, Zhiling Yan, Chujie Gao, Ruoxi Chen, Zhengqing Yuan, Yue Huang, Hanchi Sun, Jianfeng Gao, et al. Sora: A review on background, technology, limitations, and opportunities of large vision models. *arXiv preprint arXiv:2402.17177*, 2024.
- [31] Saeed Masoudnia and Reza Ebrahimpour. Mixture of experts: a literature survey. *Artificial Intelligence Review*, 42:275–293, 2014.
- [32] Chong Mou, Xintao Wang, Liangbin Xie, Yanze Wu, Jian Zhang, Zhongang Qi, and Ying Shan. T2i-adapter: Learning adapters to dig out more controllable ability for text-to-image diffusion models. In *Proceedings of the AAAI Conference on Artificial Intelligence*, volume 38, pages 4296–4304, 2024.
- [33] Yuqi Nie, Nam H Nguyen, Phanwadee Sinthong, and Jayant Kalagnanam. A time series is worth 64 words: Long-term forecasting with transformers. *arXiv preprint arXiv:2211.14730*, 2022.
- [34] Zijie Pan, Yushan Jiang, Sahil Garg, Anderson Schneider, Yuriy Nevmyvaka, and Dongjin Song. S2ip-llm: Semantic space informed prompt learning with llm for time series forecasting. *arXiv preprint arXiv:2403.05798*, 2024.

- [35] Adam Paszke, Sam Gross, Francisco Massa, Adam Lerer, James Bradbury, Gregory Chanan, Trevor Killeen, Zeming Lin, Natalia Gimelshein, Luca Antiga, et al. Pytorch: An imperative style, high-performance deep learning library. *Advances in neural information processing systems*, 32, 2019.
- [36] William Peebles and Saining Xie. Scalable diffusion models with transformers. In *Proceedings of the IEEE/CVF International Conference on Computer Vision*, pages 4195–4205, 2023.
- [37] Steve Pincus and Rudolf E Kalman. Irregularity, volatility, risk, and financial market time series. *Proceedings of the National Academy of Sciences*, 101(38):13709–13714, 2004.
- [38] Konpat Preechakul, Nattanat Chatthee, Suttisak Wizadwongsa, and Supasorn Suwajanakorn. Diffusion autoencoders: Toward a meaningful and decodable representation. In *Proceedings of the IEEE/CVF Conference on Computer Vision and Pattern Recognition*, pages 10619–10629, 2022.
- [39] Martin L Puterman. Markov decision processes. *Handbooks in operations research and management science*, 2:331–434, 1990.
- [40] Shiyu Qin, Jinpeng Wang, Yimin Zhou, Bin Chen, Tianci Luo, Baoyi An, Tao Dai, Shutao Xia, and Yaowei Wang. Mambavc: Learned visual compression with selective state spaces. *arXiv preprint arXiv:2405.15413*, 2024.
- [41] Alec Radford, Jong Wook Kim, Chris Hallacy, Aditya Ramesh, Gabriel Goh, Sandhini Agarwal, Girish Sastry, Amanda Askell, Pamela Mishkin, Jack Clark, et al. Learning transferable visual models from natural language supervision. In *International conference on machine learning*, pages 8748–8763. PMLR, 2021.
- [42] Kashif Rasul, Calvin Seward, Ingmar Schuster, and Roland Vollgraf. Autoregressive denoising diffusion models for multivariate probabilistic time series forecasting. In *International Conference on Machine Learning*, pages 8857–8868. PMLR, 2021.
- [43] Kashif Rasul, Arjun Ashok, Andrew Robert Williams, Arian Khorasani, George Adamopoulos, Rishika Bhagwatkar, Marin Biloš, Hena Ghonia, Nadhir Vincent Hassen, Anderson Schneider, et al. Lag-llama: Towards foundation models for time series forecasting. *arXiv preprint arXiv:2310.08278*, 2023.
- [44] Robin Rombach, Andreas Blattmann, Dominik Lorenz, Patrick Esser, and Björn Ommer. High-resolution image synthesis with latent diffusion models. In *Proceedings of the IEEE/CVF conference on computer vision and pattern recognition*, pages 10684–10695, 2022.
- [45] Christoph Schuhmann, Richard Vencu, Romain Beaumont, Robert Kaczmarczyk, Clayton Mullis, Aarush Katta, Theo Coombes, Jenia Jitsev, and Aran Komatsuzaki. Laion-400m: Open dataset of clip-filtered 400 million image-text pairs. *arXiv preprint arXiv:2111.02114*, 2021.
- [46] Junhong Shen, Liam Li, Lucio M Dery, Corey Staten, Mikhail Khodak, Graham Neubig, and Ameet Talwalkar. Cross-modal fine-tuning: Align then refine. In *International Conference on Machine Learning*, pages 31030–31056. PMLR, 2023.
- [47] Lifeng Shen and James Kwok. Non-autoregressive conditional diffusion models for time series prediction. In *International Conference on Machine Learning*, pages 31016–31029. PMLR, 2023.
- [48] Jascha Sohl-Dickstein, Eric Weiss, Niru Maheswaranathan, and Surya Ganguli. Deep unsupervised learning using nonequilibrium thermodynamics. In *International conference on machine learning*, pages 2256–2265. PMLR, 2015.
- [49] Jiaming Song, Chenlin Meng, and Stefano Ermon. Denoising diffusion implicit models. *arXiv preprint arXiv:2010.02502*, 2020.
- [50] Yang Song, Jascha Sohl-Dickstein, Diederik P Kingma, Abhishek Kumar, Stefano Ermon, and Ben Poole. Score-based generative modeling through stochastic differential equations. *arXiv preprint arXiv:2011.13456*, 2020.

- [51] Krishna Srinivasan, Karthik Raman, Jiecao Chen, Michael Bendersky, and Marc Najork. Wit: Wikipedia-based image text dataset for multimodal multilingual machine learning. In *Proceedings of the 44th International ACM SIGIR Conference on Research and Development in Information Retrieval*, pages 2443–2449, 2021.
- [52] Stefano Frizzo Stefenon, Laio Oriel Seman, Viviana Cocco Mariani, and Leandro dos Santos Coelho. Aggregating prophet and seasonal trend decomposition for time series forecasting of italian electricity spot prices. *Energies*, 16(3):1371, 2023.
- [53] Yusuke Tashiro, Jiaming Song, Yang Song, and Stefano Ermon. Csd: Conditional score-based diffusion models for probabilistic time series imputation. *Advances in Neural Information Processing Systems*, 34:24804–24816, 2021.
- [54] Hugo Touvron, Thibaut Lavril, Gautier Izacard, Xavier Martinet, Marie-Anne Lachaux, Timothée Lacroix, Baptiste Rozière, Naman Goyal, Eric Hambro, Faisal Azhar, et al. Llama: Open and efficient foundation language models. *arXiv preprint arXiv:2302.13971*, 2023.
- [55] Artur Trindade. ElectricityLoadDiagrams20112014. UCI Machine Learning Repository, 2015. DOI: <https://doi.org/10.24432/C58C86>.
- [56] Jan Philip Wahle, Terry Ruas, Tomáš Foltýnek, Norman Meuschke, and Bela Gipp. Identifying machine-paraphrased plagiarism. In *International Conference on Information*, pages 393–413. Springer, 2022.
- [57] Jianyi Wang, Zongsheng Yue, Shangchen Zhou, Kelvin CK Chan, and Chen Change Loy. Exploiting diffusion prior for real-world image super-resolution. *arXiv preprint arXiv:2305.07015*, 2023.
- [58] Haomin Wen, Youfang Lin, Yutong Xia, Huaiyu Wan, Qingsong Wen, Roger Zimmermann, and Yuxuan Liang. Diffstg: Probabilistic spatio-temporal graph forecasting with denoising diffusion models. In *Proceedings of the 31st ACM International Conference on Advances in Geographic Information Systems*, pages 1–12, 2023.
- [59] Haixu Wu, Jiehui Xu, Jianmin Wang, and Mingsheng Long. Autoformer: Decomposition transformers with auto-correlation for long-term series forecasting. *Advances in neural information processing systems*, 34:22419–22430, 2021.
- [60] Haixu Wu, Tengge Hu, Yong Liu, Hang Zhou, Jianmin Wang, and Mingsheng Long. Timesnet: Temporal 2d-variation modeling for general time series analysis. In *The eleventh international conference on learning representations*, 2022.
- [61] Robert Alan Yaffee and Monnie McGee. *An introduction to time series analysis and forecasting: with applications of SAS® and SPSS®*. Elsevier, 2000.
- [62] Tijin Yan, Hongwei Zhang, Tong Zhou, Yufeng Zhan, and Yuanqing Xia. Scoregrad: Multivariate probabilistic time series forecasting with continuous energy-based generative models. *arXiv preprint arXiv:2106.10121*, 2021.
- [63] Xinyu Yuan and Yan Qiao. Diffusion-ts: Interpretable diffusion for general time series generation. *arXiv preprint arXiv:2403.01742*, 2024.
- [64] Ailing Zeng, Muxi Chen, Lei Zhang, and Qiang Xu. Are transformers effective for time series forecasting? In *Proceedings of the AAAI conference on artificial intelligence*, volume 37, pages 11121–11128, 2023.
- [65] Lvmin Zhang, Anyi Rao, and Maneesh Agrawala. Adding conditional control to text-to-image diffusion models. In *Proceedings of the IEEE/CVF International Conference on Computer Vision*, pages 3836–3847, 2023.
- [66] Shihao Zhao, Dongdong Chen, Yen-Chun Chen, Jianmin Bao, Shaozhe Hao, Lu Yuan, and Kwan-Yee K Wong. Uni-controlnet: All-in-one control to text-to-image diffusion models. *Advances in Neural Information Processing Systems*, 36, 2024.

- [67] Haoyi Zhou, Shanghang Zhang, Jieqi Peng, Shuai Zhang, Jianxin Li, Hui Xiong, and Wancai Zhang. Informer: Beyond efficient transformer for long sequence time-series forecasting. In *Proceedings of the AAAI conference on artificial intelligence*, volume 35, pages 11106–11115, 2021.
- [68] Tian Zhou, Ziqing Ma, Qingsong Wen, Xue Wang, Liang Sun, and Rong Jin. Fedformer: Frequency enhanced decomposed transformer for long-term series forecasting. In *International conference on machine learning*, pages 27268–27286. PMLR, 2022.
- [69] Tian Zhou, Peisong Niu, Liang Sun, Rong Jin, et al. One fits all: Power general time series analysis by pretrained lm. *Advances in neural information processing systems*, 36:43322–43355, 2023.

A Expectation

We have validated the potential of the Generative Pre-trained Diffusion (GPD) paradigm as a zero-shot forecaster. In the Appendix, we further verify its capabilities in zero-shot imputation and classification. We have thoroughly explored the effectiveness and superiority of the GPD paradigm using a simple baseline network. Our aim is to lay the groundwork for foundation models in time series. In fact, we can pretrain a unified model, similar to cross-domain, to accomplish most downstream tasks. Extensive experiments demonstrate the feasibility of the GPD paradigm. We introduce many interesting points worthy of further follow-up and research. Code can be accessed from anonymous link <https://anonymous.4open.science/r/GPD>.

B Zero-Shot Imputation

Time series imputation under the GPD paradigm is similar to time series forecasting. We also rely on a pre-trained model without fine-tuning. Given a sequence Y with missing data, where the part of missing values can be considered as a mask M . We can use the non-missing data as prompts to align the distribution according to the method introduced in Section 2.3. The imputation task can be completed simply by embedding the prompts according to the following formula:

$$X_{t-1} = \{x_{t-1}^i\}_{i=1}^L * (1 - M) + \{y_{t-1}^i\}_{i=1}^L * M \quad (8)$$

where, X_{t-1} is the posterior distribution of the t -th step in the reverse diffusion process, and L represents the length of the entire sequence. We illustrate the imputation visualization with ratios of 30%, 60%, 90% in Fig. 8. Our method demonstrates excellent performance even with 90% of the values missing. Note that for additional downstream tasks, we do not introduce additional learning. Instead, we rely on the strong generalization and zero-shot capabilities of the GPD paradigm. Compared to end-to-end modeling methods, generative pre-training paradigms show more potential to become foundation models for time series.

C Zero-Shot Classification

Li et al. [24] propose that diffusion models can serve as zero-shot classifiers. Following their method, we validate the zero-shot capability of GPD in classification task. Note that Li et al. [24] build upon multi-modal diffusion models, utilizing specific category text to modulate diffusion errors. Since GPD is not based on multimodality, we propose some enhancements and conduct simple binary classification experiments. We consider models trained on a single domain as experts in a Mixture of Experts (MoE [31, 18]), each proficient in specific domain knowledge. Specifically, pre-trained models based on long-range forecasting on the ETTh1 and Weather datasets perform classification experiments. Given a test sequence $Y_0 \in \{\text{ETTh1, Weather}\}$, we perform forward diffusion with reparameterization to add noise:

$$Y_t = \sqrt{\bar{\alpha}_t} Y_0 + \sqrt{1 - \bar{\alpha}_t} \epsilon \quad (9)$$

Then, we utilize these two pre-trained models to obtain predicted noise (ϵ_θ^E and ϵ_θ^W) at each time step. Subsequently, following Li et al.'s error computation method, we obtain the diffusion errors $E_E = \min(\text{Errors}_E)$ and $E_W = \min(\text{Errors}_W)$. The classification result for a specific domain is determined by the smaller domain error $\min([E_E, E_W])$. We randomly sample 1000 time series from the testset of ETTh1 and Weather for evaluation. The classification accuracy on both datasets exceeds 90%.

D More Experimental Details

All our experiments are conducted in a completely fair manner. The only difference lies in the batch size settings. Since our model is smaller, we can use larger batch sizes for testing. The historical length settings in different works [29, 33, 19] result in different lengths of the testset. So we calculate the length of their testsets beforehand and adjust our batch size to ensure consistency in testset length. For instance, on the ETTh1 dataset with a historical length of 512 and a prediction length of 712, their testset length is 2161, thereby we set our batch size to 2161.

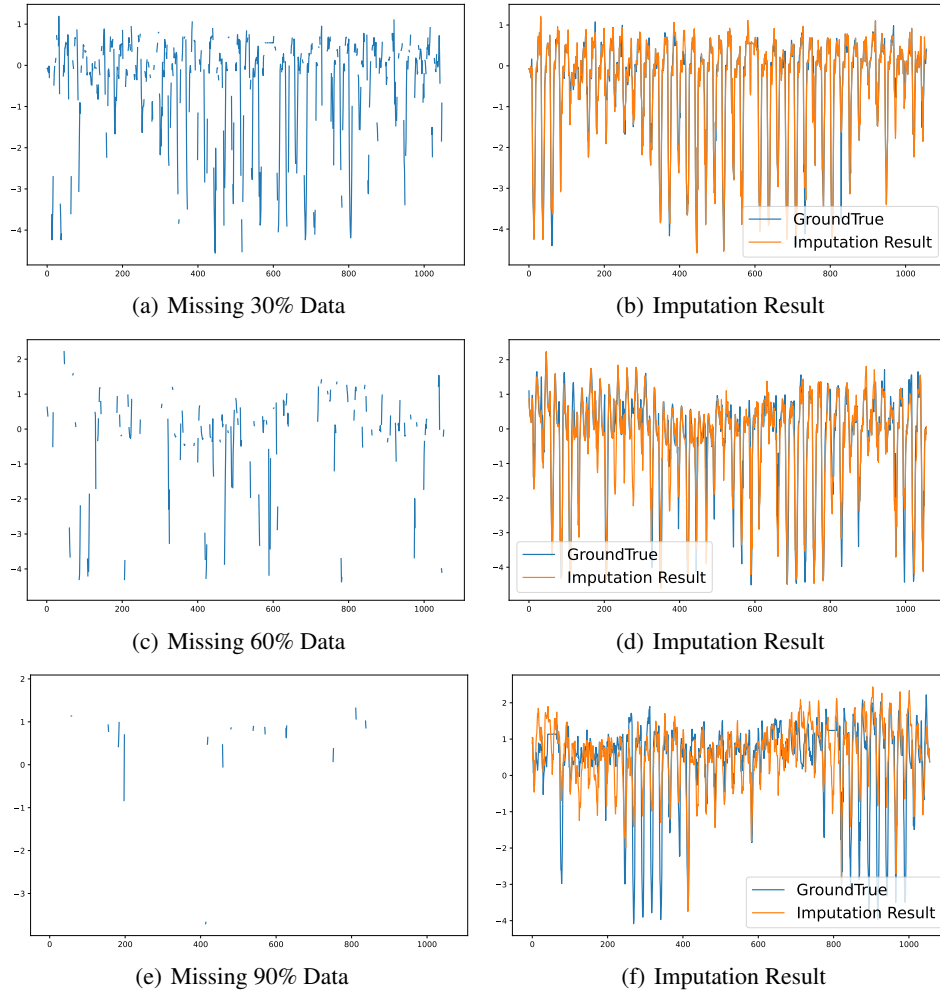


Figure 8: Visualization of Imputation Results.

E Visualization

The forecasting results of pure generative models exhibit non-uniqueness. Therefore, we display the median, 50%, and 90% distribution intervals of 100 samples in Fig. 9. Simultaneously, we present visual comparisons of sampling instance normalization (SIN) against results without normalization. As shown in Fig. 9, the uncertainty of SIN is greater, compared to when no normalization is applied, hence it tends to predict more boldly in the face of abrupt trends.

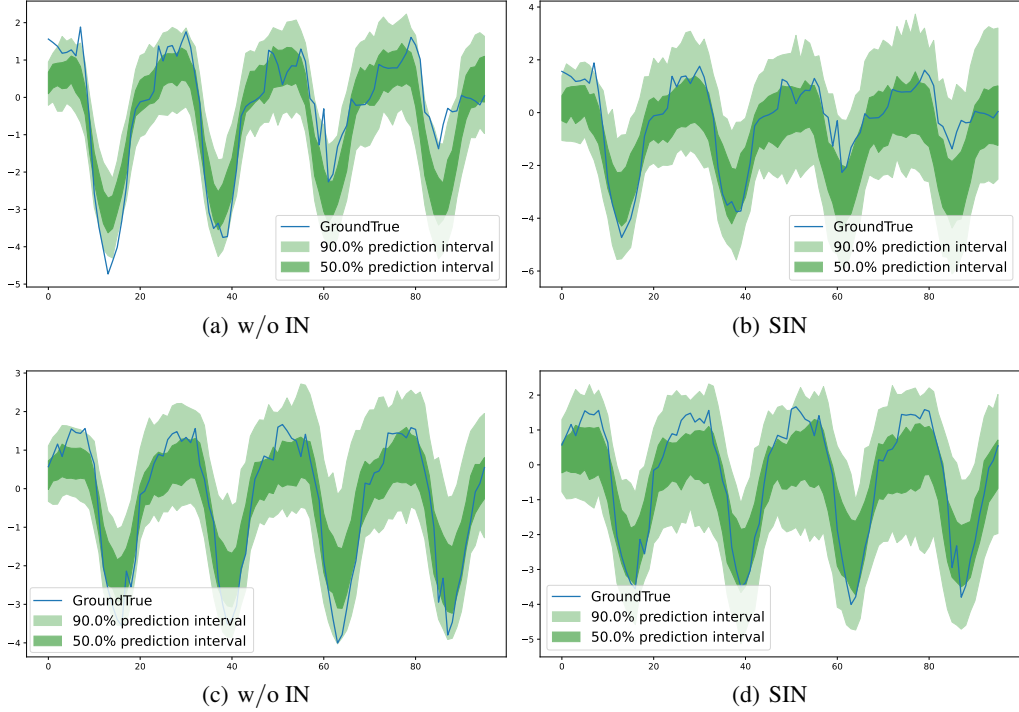


Figure 9: Visualization comparison of predicted distributions for sampling instance normalization (SIN) and without instance normalization (w/o IN).

Table 7: **Full long-term forecasting results.** A lower value indicates better performance. **Red** and **blue** indicates the best and the second best performance.

Methods	Ours		TimeLLM		LLM4TS		GPT4TS		DLinear		PatchTST		FEDformer		Autoformer		Informer		Pyraformer		
Metric	MSE	MAE	MSE	MAE	MSE	MAE	MSE	MAE	MSE	MAE	MSE	MAE	MSE	MAE	MSE	MAE	MSE	MAE	MSE	MAE	
ETTh1	96	0.350	0.390	0.362	0.392	0.371	0.394	0.376	0.397	0.375	0.399	0.370	0.399	0.376	0.419	0.449	0.459	0.865	0.713	0.664	0.612
	192	0.375	0.409	0.398	0.418	0.403	0.412	0.416	0.418	0.405	0.416	0.413	0.421	0.420	0.448	0.500	0.482	1.008	0.792	0.790	0.681
	336	0.390	0.424	0.430	0.427	0.420	0.422	0.442	0.433	0.439	0.443	0.422	0.436	0.459	0.465	0.521	0.496	1.107	0.809	0.891	0.738
	720	0.450	0.467	0.442	0.457	0.422	0.444	0.477	0.456	0.472	0.492	0.447	0.466	0.506	0.507	0.514	0.512	1.181	0.865	0.963	0.782
	Avg	0.391	0.423	0.408	0.423	0.404	0.418	0.428	0.426	0.423	0.438	0.413	0.461	0.440	0.677	0.496	0.487	1.040	0.795	0.827	0.703
ETTh2	96	0.237	0.316	0.268	0.328	0.262	0.332	0.285	0.342	0.289	0.353	0.274	0.336	0.358	0.397	0.346	0.388	3.755	1.525	0.645	0.597
	192	0.272	0.344	0.329	0.375	0.328	0.377	0.354	0.389	0.383	0.418	0.339	0.379	0.429	0.439	0.456	0.452	5.602	1.931	0.799	0.683
	336	0.297	0.366	0.368	0.409	0.353	0.396	0.373	0.407	0.448	0.465	0.329	0.380	0.496	0.487	0.482	0.486	4.721	1.835	0.907	0.747
	720	0.394	0.434	0.372	0.420	0.383	0.425	0.406	0.441	0.605	0.551	0.379	0.422	0.463	0.474	0.515	0.511	3.647	1.625	0.963	0.783
	Avg	0.300	0.365	0.334	0.383	0.331	0.383	0.355	0.395	0.431	0.447	0.370	0.379	0.437	0.449	0.450	0.459	4.431	1.729	0.829	0.703
ETTh1	96	0.288	0.340	0.272	0.334	0.285	0.343	0.292	0.346	0.299	0.343	0.290	0.342	0.379	0.419	0.505	0.475	0.672	0.571	0.543	0.510
	192	0.325	0.363	0.310	0.358	0.324	0.366	0.332	0.372	0.335	0.365	0.332	0.369	0.426	0.441	0.553	0.496	0.795	0.669	0.557	0.537
	336	0.363	0.386	0.352	0.384	0.353	0.385	0.366	0.394	0.369	0.386	0.366	0.392	0.445	0.459	0.621	0.537	1.212	0.871	0.754	0.655
	720	0.421	0.418	0.383	0.411	0.408	0.419	0.417	0.421	0.425	0.421	0.416	0.420	0.543	0.490	0.671	0.561	1.166	0.823	0.908	0.724
	Avg	0.349	0.377	0.329	0.372	0.343	0.378	0.352	0.383	0.357	0.379	0.351	0.381	0.448	0.452	0.588	0.517	0.961	0.734	0.691	0.607
ETTh2	96	0.168	0.253	0.161	0.253	0.165	0.254	0.173	0.262	0.167	0.269	0.165	0.255	0.203	0.287	0.255	0.339	0.365	0.453	0.435	0.507
	192	0.227	0.292	0.219	0.293	0.220	0.292	0.229	0.301	0.224	0.303	0.220	0.292	0.269	0.328	0.281	0.340	0.533	0.563	0.730	0.673
	336	0.282	0.327	0.271	0.329	0.268	0.326	0.286	0.341	0.281	0.342	0.274	0.329	0.325	0.366	0.339	0.372	1.363	0.887	1.201	0.845
	720	0.372	0.385	0.352	0.379	0.350	0.380	0.378	0.401	0.397	0.421	0.362	0.385	0.421	0.415	0.433	0.432	3.379	1.338	3.625	1.451
	Avg	0.262	0.314	0.251	0.313	0.251	0.313	0.267	0.326	0.267	0.334	0.255	0.315	0.305	0.349	0.327	0.371	1.410	0.810	1.498	0.869
Weather	96	0.159	0.221	0.147	0.201	0.147	0.196	0.162	0.212	0.176	0.237	0.149	0.198	0.217	0.296	0.266	0.336	0.300	0.384	0.896	0.556
	192	0.204	0.267	0.189	0.234	0.191	0.238	0.204	0.248	0.220	0.282	0.194	0.241	0.276	0.336	0.307	0.367	0.598	0.434	0.622	0.624
	336	0.252	0.309	0.262	0.279	0.241	0.277	0.254	0.286	0.265	0.319	0.245	0.282	0.339	0.380	0.359	0.395	0.578	0.523	0.739	0.753
	720	0.322	0.362	0.304	0.316	0.313	0.329	0.326	0.337	0.333	0.362	0.314	0.334	0.403	0.428	0.419	0.428	1.059	0.741	1.004	0.934
	Avg	0.234	0.289	0.225	0.257	0.223	0.260	0.237	0.271	0.249	0.300	0.226	0.264	0.310	0.360	0.338	0.382	0.634	0.521	0.815	0.717
Electricity	96	0.128	0.238	0.131	0.224	0.128	0.223	0.139	0.238	0.140	0.237	0.139	0.222	0.193	0.308	0.201	0.317	0.274	0.368	0.386	0.449
	192	0.148	0.258	0.152	0.241	0.146	0.240	0.153	0.251	0.153	0.249	0.157	0.240	0.201	0.315	0.222	0.334	0.296	0.386	0.386	0.443
	336	0.169	0.279	0.160	0.248	0.163	0.258	0.169	0.266	0.169	0.267	0.163	0.259	0.214	0.329	0.231	0.338	0.300	0.394	0.378	0.443
	720	0.214	0.317	0.192	0.298	0.200	0.292	0.206	0.297	0.203	0.301	0.197	0.290	0.246	0.355	0.254	0.361	0.373	0.439	0.376	0.445
	Avg	0.165	0.273	0.158	0.252	0.159	0.253	0.167	0.263	0.166	0.264	0.164	0.253	0.214	0.327	0.227	0.338	0.311	0.397	0.382	0.445
Traffic	96	0.359	0.260	0.362	0.248	0.372	0.259	0.388	0.282	0.420	0.282	0.360	0.249	0.587	0.366	0.613	0.388	0.719	0.391	2.085	0.468
	192	0.373	0.267	0.374	0.247	0.391	0.265	0.407	0.290	0.424	0.287	0.379	0.256	0.604	0.373	0.616	0.382	0.696	0.379	0.867	0.467
	336	0.399	0.282	0.385	0.271	0.405	0.275	0.412	0.294	0.436	0.296	0.392	0.264	0.621	0.383	0.622	0.337	0.777	0.420	0.869	0.469
	720	0.440	0.305	0.430	0.288	0.437	0.292	0.450	0.312	0.466	0.315	0.432	0.286	0.626	0.382	0.660	0.408	0.864	0.472	0.881	0.473
	Avg	0.393	0.279	0.388	0.264	0.401	0.273	0.414	0.295	0.437	0.264	0.391	0.264	0.611	0.376	0.628	0.379	0.764	0.416	1.176	0.469

Table 8: **Full zero-shot learning results on ETT datasets.** A lower value indicates better performance. **Red** and **blue** indicates the best and the second best performance.

Methods		Ours		TimeLLM		LLMTime		GPT4TS		DLinear		PatchTST		TimesNet		Autoformer	
Metric		MSE	MAE	MSE	MAE	MSE	MAE	MSE	MAE	MSE	MAE	MSE	MAE	MSE	MAE	MSE	MAE
ETTh1 → ETTh2	96	0.239	0.321	0.279	0.337	0.510	0.576	0.335	0.374	0.347	0.400	0.304	0.350	0.358	0.387	0.469	0.486
	192	0.275	0.349	0.351	0.374	0.523	0.586	0.412	0.417	0.447	0.460	0.386	0.400	0.427	0.429	0.634	0.567
	336	0.301	0.371	0.388	0.415	0.640	0.637	0.441	0.444	0.515	0.505	0.414	0.428	0.449	0.451	0.655	0.588
	720	0.396	0.432	0.391	0.420	2.296	1.034	0.438	0.452	0.665	0.589	0.419	0.443	0.448	0.458	0.570	0.549
	Avg	0.303	0.368	0.353	0.387	0.992	0.708	0.406	0.422	0.493	0.488	0.380	0.405	0.421	0.431	0.582	0.548
ETTh1 → ETTm2	96	0.224	0.316	0.189	0.293	0.646	0.563	0.236	0.315	0.255	0.357	0.215	0.304	0.239	0.313	0.352	0.432
	192	0.279	0.349	0.237	0.312	0.934	0.654	0.287	0.342	0.338	0.413	0.275	0.339	0.291	0.342	0.413	0.460
	336	0.329	0.377	0.291	0.365	1.157	0.728	0.341	0.374	0.425	0.465	0.334	0.373	0.342	0.371	0.465	0.489
	720	0.413	0.426	0.372	0.390	4.730	1.531	0.435	0.422	0.640	0.573	0.431	0.424	0.434	0.419	0.599	0.551
	Avg	0.311	0.367	0.273	0.340	1.867	0.869	0.325	0.363	0.415	0.452	0.314	0.360	0.327	0.361	0.457	0.483
ETTh2 → ETTh1	96	0.394	0.421	0.450	0.452	1.130	0.777	0.732	0.577	0.689	0.555	0.485	0.465	0.848	0.601	0.693	0.569
	192	0.426	0.439	0.465	0.461	1.242	0.820	0.758	0.559	0.707	0.568	0.565	0.509	0.860	0.610	0.760	0.601
	336	0.455	0.459	0.501	0.482	1.328	0.864	0.759	0.578	0.710	0.577	0.581	0.515	0.867	0.626	0.781	0.619
	720	0.510	0.505	0.501	0.502	4.145	1.461	0.781	0.597	0.704	0.596	0.628	0.561	0.887	0.648	0.796	0.644
	Avg	0.446	0.456	0.479	0.474	1.961	0.981	0.757	0.578	0.703	0.574	0.565	0.513	0.865	0.621	0.757	0.608
ETTh2 → ETTm2	96	0.219	0.306	0.174	0.276	0.646	0.563	0.253	0.329	0.240	0.336	0.226	0.309	0.248	0.324	0.263	0.352
	192	0.280	0.343	0.233	0.315	0.934	0.654	0.293	0.346	0.295	0.369	0.289	0.345	0.296	0.352	0.326	0.389
	336	0.335	0.376	0.291	0.337	1.157	0.728	0.347	0.376	0.345	0.397	0.348	0.379	0.353	0.383	0.387	0.426
	720	0.429	0.430	0.392	0.417	4.730	1.531	0.446	0.429	0.432	0.442	0.439	0.427	0.471	0.446	0.487	0.478
	Avg	0.316	0.364	0.272	0.341	1.867	0.869	0.335	0.370	0.328	0.386	0.325	0.365	0.342	0.376	0.366	0.411
ETTh1 → ETTm1	96	0.280	0.348	0.321	0.369	0.510	0.576	0.353	0.392	0.365	0.415	0.354	0.385	0.377	0.407	0.435	0.470
	192	0.314	0.375	0.389	0.410	0.523	0.586	0.443	0.437	0.454	0.462	0.447	0.434	0.471	0.453	0.495	0.489
	336	0.332	0.393	0.408	0.433	0.640	0.637	0.469	0.461	0.496	0.494	0.481	0.463	0.472	0.484	0.470	0.472
	720	0.404	0.439	0.406	0.436	2.296	1.034	0.466	0.468	0.541	0.529	0.474	0.471	0.495	0.482	0.480	0.485
	Avg	0.333	0.389	0.381	0.412	0.992	0.708	0.433	0.439	0.464	0.475	0.439	0.438	0.457	0.454	0.470	0.479
ETTh1 → ETTm2	96	0.179	0.260	0.169	0.257	0.646	0.563	0.217	0.294	0.221	0.314	0.195	0.271	0.222	0.295	0.385	0.457
	192	0.231	0.293	0.227	0.318	0.934	0.654	0.277	0.327	0.286	0.359	0.258	0.311	0.288	0.337	0.433	0.469
	336	0.288	0.332	0.290	0.338	1.157	0.728	0.331	0.360	0.357	0.406	0.317	0.348	0.341	0.367	0.476	0.477
	720	0.367	0.381	0.375	0.367	4.730	1.531	0.429	0.413	0.476	0.476	0.416	0.404	0.436	0.418	0.582	0.535
	Avg	0.266	0.317	0.268	0.320	1.867	0.869	0.313	0.348	0.335	0.389	0.296	0.334	0.322	0.354	0.469	0.484
ETTh2 → ETTm2	96	0.253	0.325	0.298	0.356	0.510	0.576	0.360	0.401	0.333	0.391	0.327	0.367	0.360	0.401	0.353	0.393
	192	0.289	0.353	0.359	0.397	0.523	0.586	0.434	0.437	0.441	0.456	0.411	0.418	0.434	0.437	0.432	0.437
	336	0.313	0.375	0.367	0.412	0.640	0.637	0.460	0.459	0.505	0.503	0.439	0.447	0.460	0.459	0.452	0.459
	720	0.384	0.422	0.393	0.434	2.296	1.034	0.485	0.477	0.543	0.534	0.459	0.470	0.485	0.477	0.453	0.467
	Avg	0.311	0.369	0.354	0.400	0.992	0.708	0.435	0.443	0.455	0.471	0.409	0.425	0.435	0.443	0.423	0.439
ETTh2 → ETTm1	96	0.345	0.380	0.359	0.397	1.179	0.781	0.747	0.558	0.570	0.490	0.491	0.437	0.747	0.558	0.735	0.576
	192	0.364	0.393	0.390	0.420	1.327	0.846	0.781	0.560	0.590	0.506	0.530	0.470	0.781	0.560	0.753	0.586
	336	0.390	0.407	0.421	0.445	1.478	0.902	0.778	0.578	0.706	0.567	0.565	0.497	0.778	0.578	0.750	0.593
	720	0.437	0.434	0.487	0.488	3.749	1.408	0.769	0.573	0.731	0.584	0.686	0.565	0.769	0.573	0.782	0.609
	Avg	0.384	0.404	0.414	0.438	1.933	0.984	0.769	0.567	0.649	0.537	0.568	0.492	0.769	0.567	0.755	0.591

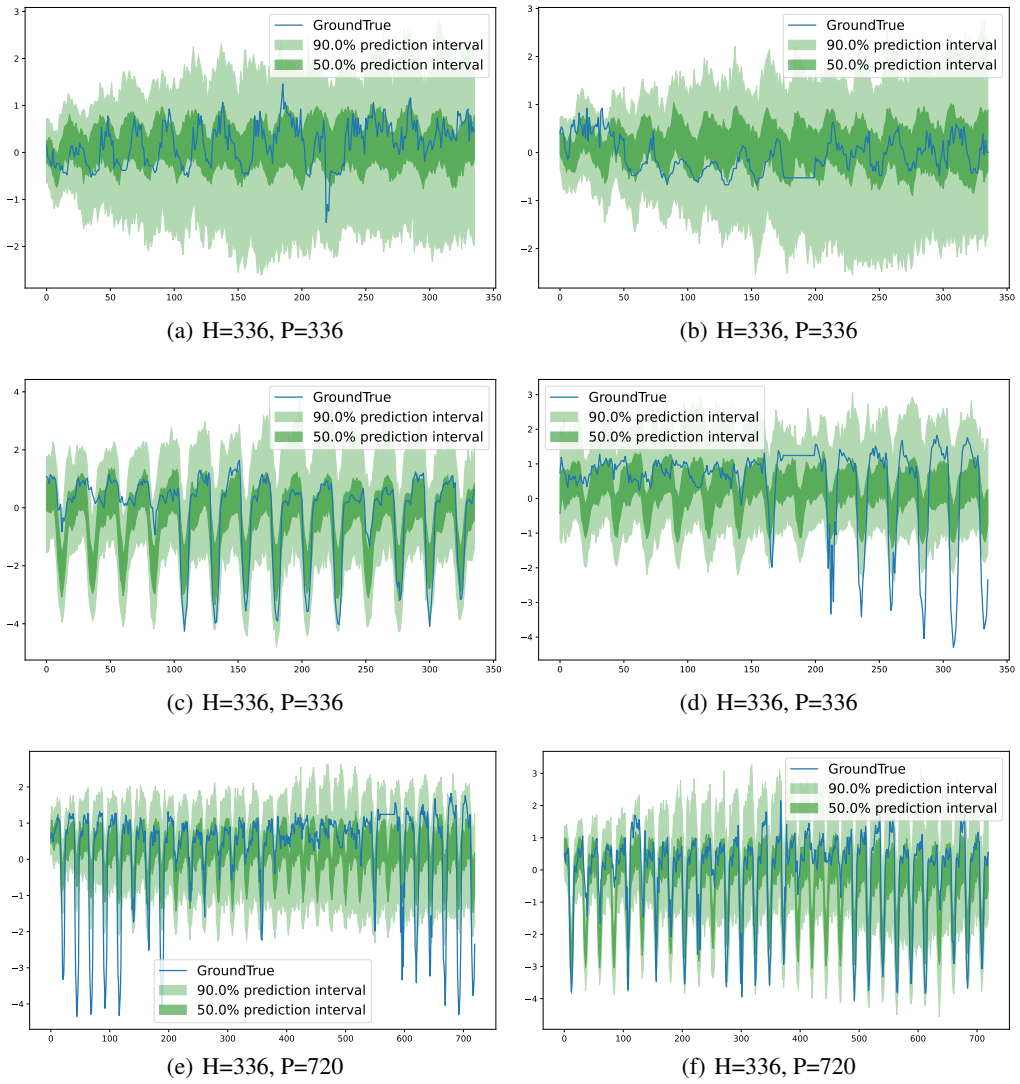


Figure 10: More Results